Available online at www.sciencedirect.com

ScienceDirect

Procedia Computer Science 200 (2022) 49–61

Procedia Computer Science

www.elsevier.com/locate/procedia

3rd International Conference on Industry 4.0 and Smart Manufacturing

Interactive Sensor Dashboard for Smart Manufacturing

Somnath Arjun, LRD Murthy, Pradipta Biswas*

Indian Institute of Science, Bangalore, India
pradipta@iisc.ac.in

Abstract

This paper presents a smart sensor dashboard for a digital twin of a smart manufacturing workshop. We described the development of the digital twin followed by three user studies on the visualization and interaction aspects of the smart sensor dashboard. The first two user studies evaluated ocular parameters and users' response for different 2D and 3D graphs rendered on 2D screen and VR headset. The bar chart found to generate most accurate users' response in both 2D and 3D case. The third study recreated the Fitts' Law task in 3D and compared visual and haptic feedback. We found that haptic feedback significantly improved quantitative metrics of interaction than a no-feedback case, whereas multimodal feedback is significantly improved qualitative metrics of the interaction. Results from the study can be utilized to design VR environments with interactive graphs.

Keywords: Information Visualization; Eye Tracking; Sensor netwrok; Interaction; Virtual Reality.

1. Introduction

Visualizing and interacting with large-scale data is an open problem in the context of information visualization. For example, let us consider a smart factory spread over several buildings and workshops, each containing several environment monitoring sensors. Visualizing these sensors' information over a time period and for each sensor separately requires a large amount of screen estate. Additionally, users may require interacting with this data to infer key performance objectives like productivity, pollution level, and safety which adds more challenge to the visualization platform. Existing visualization techniques for smart manufacturing explored the relationship among data by

* Corresponding author. Tel.: +0-000-000-0000 ; fax: +0-000-000-0000 .
E-mail address: author@institute.xxx

10.1016/j.procs.2022.01.204

establishing ontologies and visualizing network diagrams among different items in・・ [1], [2]. Sackett, Al-Gaylani, Tiwari, & Williams [3] reviewed existing visualization techniques but did not provide detail on visualizing both temporal and spatial information simultaneously. Existing smart manufacturing set up at Cranfield and Sheffield universities are exploring using state-of-the-art Virtual Reality (VR), augmented reality, and projected displays (e.g., Microsoft HoloLens) to explain individual components or working principles of complex machines. Existing smart manufacturing processes investigate large touchscreen (e.g., Clevertouch Plus) and different VR systems for visualization, although those are not exclusively used to visualize sensor data. Existing augmented reality systems mostly use a tablet computer to zoom in small circuit elements or showing descriptions of individual components but not for helping sensor fusion or visualization of sensor data.

Our research is addressing large scale sensor visualization and interaction from the following three facets

- Investigating different topology and network options to connect multiple sensors to visualization module.
- Developing a 2-dimensional sensor dashboard and evaluating different visualization strategies by analyzing the eye gaze of users.
- Developing a 3-D digital twin with embedded IoT modules showing sensor data and investigating multimodal interaction with the VR system.

The paper is organized as follows. The following section presents a brief literature survey followed by a description of the three modules presented above. Section IV presents two user studies followed by concluding remarks.

2. Literature Survey

Sensor data are time-series data that typically have more than three dimensions. Visualizing high-dimensional data is an active research area, and the visualization community has been researching this field for the past three decades. Visualization is an extensive process with a sequence of stages that can be studied independently in terms of algorithms, data abstraction, and geometry [14]. The physical limitations of display devices and our visual systems prevent the direct display and rapid recognition of data with dimensions higher than two or three. The visualization process starts with the raw data that will be potentially visualized. In the past, a broad number of approaches like PCA [4], MDS [5] have been introduced to visually convey high-dimensional information by transforming them to low dimensional projections or abstract representations. The next stage of the visualization pipeline involves mapping components of the data record to the features of graphical attributes. Techniques such as non-projective mapping between n-dimensional and 2-dimensional sets like parallel coordinates [6] and faces to represent points in k-dimensional space graphically [7] were introduced. The last stage of visualization is the rendering process that generates images in the screen space. Clutter reduction [8] is one of the several efforts that have been made for this stage of visualization. Research that is focused on high-dimensional data visualization [13] falls in one of the three stages of visualization, for instance, visual data mining [9], quality measures [10,11,12]. Visualization and interactive tools have been developed to identify and understand clusters and complex patterns in high-dimensional data. SMARTexplore [15] is one such example that introduces a novel visual analytics technique that simplifies the identification and understanding of clusters, correlations, and complex patterns in high-dimensional data.

In recent times with the advancement of interactive devices, the visualization process also changed from a one-way rendering system to an interactive system allowing users to interact with data to interpret it at various stages of aggregation. For example, in our daily lives, we interact with a map application in our smartphone through multiple modalities like multi-touch, gesture, speech recognition. Richard Bolt's "Put That There" [16] system first demonstrated the importance of multimodal interfaces. Later, numerous systems [17,18,19] integrated various input modalities like speech, gesture, pen input. Even though the modalities like speech, graphics, virtual characters were explored for output, relatively less work has happened on the multimodal output front, which focuses on how the systems should respond to user actions. In VR, where an entirely virtual environment can provide an immersive experience visually, other sensations that humans can feel in the real world like tactile responses, environmental sensations like temperature and pressure are inherently not present. Hence, the design of multimodal output in VR must be studied with a wide range of contexts and applications. Erler・ [20] studied the effect of haptic and visual feedback on a task involving grabbing and throwing a VR basketball game using the controller. It was found that the presence of feedback compared to no-feedback improved accuracy and predictability, but no difference was reported in task load and usability. They also noted that releasing a button on the controller is a bad metaphor for releasing a grabbed virtual object.

3. Proposed Approach

We applied four approaches that are described below.

3.1. IOT Nodes

Our proposed visualization system (Figure 1) consists of the following three parts

- IoT unit with a single-board computer
- An interactive visualization module
- An early warning system

Each IoT node consists of a single-board computer and a set of sensors. The single-board computer records data from different sensors and fuses sensor signals when required. Presently, we developed the IoT node for environment tracking using MQ-5 Smoke Sensor, HL-83 Flood / Rain Sensor, and a DS18B20 temperature sensor. The visualization module runs on a standard desktop or laptop computer attached to a screen. The next section describes the different 2D visualization techniques explored so far. The visualization module is integrated into an analytics and alert module that constantly analyses sensor data and sets out an alert if any values cross a threshold. The user can send either a manual alert or set up an automatic alert for all or a subset of sensors using the graphical user interface provided with the visualization module. The alert is sent as a Gmail to a pre-recorded email address. We chose Gmail as an alert platform as sending an SMS requires the visualization module to be integrated with a telephone communication unit, while social networking messages (like Facebook or WhatsApp alert) require the end-user to subscribe to a social networking site. Gmail can be received on a smartphone or smartwatch. The Gmail message summarizes sensor readings and has a subject stating the type of sensor creating the alert. More details on the system can be found in a separate paper [21], and a video demonstration of the system can be found at https://youtu.be/FX8zfQE5GF8.

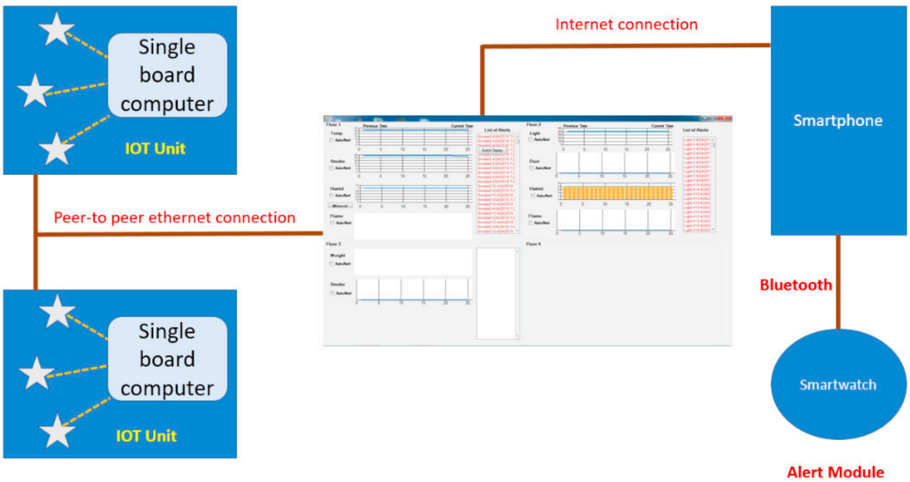

Fig. 1 Different modules of the system

3.2. 2D Visualization

Initially, we undertook a study to investigate how users interpret information from different graphs [22]. Software consisting of four visualization techniques and a set of five questions with multiple choice answers were developed. Users were asked to answer the set of questions as a part of the task. We captured gaze locations using an eye tracker for analyzing users' attention on parts of the graphs. We analyzed gaze data using the Expectation-Maximization algorithm. Results of the study show that the bar graph has the highest accuracy and the area graph has the lowest response time while performing the task. Based on the results, we developed a two-dimensional interface that can help to visualize high-dimensional data with high accuracy and lower response time. In our new visualization system, the circle of the scatter plots represents the area where the sensors are located, and the bars represent the values of the sensors over a period of time. Figure 2 shows a sample interface of the software developed for the study and the new 2D visualization technique. We also undertook a user study on 3D visualization techniques described in the next section.

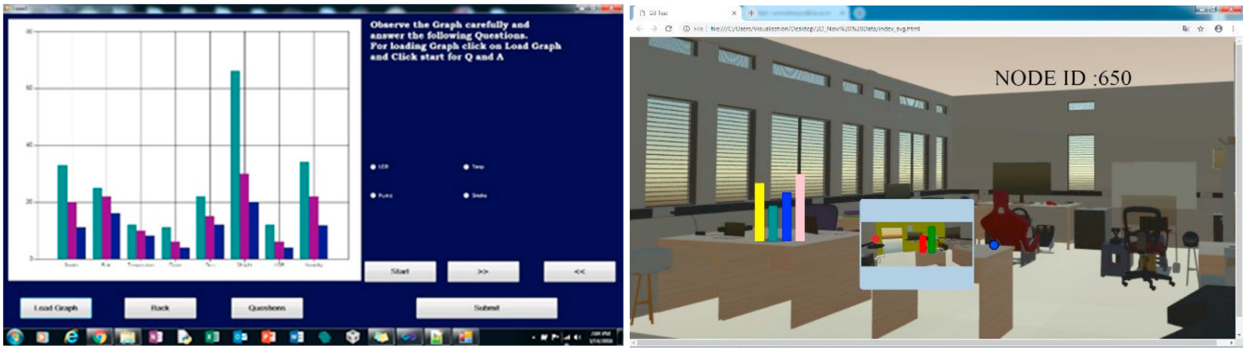

Fig. 2 Bar graph and two-dimensional visualisation

3.3. 3D Visualization

We undertook a study for comparing graphical primitives of 3D charts in a VR environment. Visualization can be termed as a collection of graphical objects. There are eight ways in which graphical objects can encode information, i.e., eight visual variables – position, shape, size, opacity, color, orientation, texture, and motion. These eight variables can be adjusted as necessary to maximize the effectiveness of visualization to convey information. We compared six different 3D graphs involving two graph types and five visual variables. We recorded and calculated gaze-based metrics. Furthermore, we calculated cognitive load from ocular parameters. The VR scene is shown in figure 3.

Fig. 3 Virtual Reality scene

3.4. VR Digital Twin

We assumed that the 3D visualization would provide an extra dimension to the view and allow users to interact naturally. We aimed to study and understand its efficacy when compared to 2D visualization. We chose VR as the platform for creating a 3D digital twin for a smart factory. A walk-through of the large manufacturing setup across all floors would also address the interaction, and the screen estate issues mentioned earlier and provided 3D visualization. We integrated an ambient light sensor (BH1750) and, temperature and humidity sensor (DHT22) to show a real-time visualization of the data stream(s) in a VR setup. Both sensors provide a digital output. The BH1750 sensor has a built-in 16-bit A2D converter, and the output unit is lux. The DHT22 sensor provides temperature in Celsius and humidity as a relative percentage. Sensors are interfaced with the VR machine through their respective wireless module(s) [24]. After establishing a peer-to-peer connection, an individual wireless module communicates with a VR machine using UDP protocol at a frequency of 1 Hz. The data stream taken from the light sensor is visualized as an area graph [25] (Figure 4). The graph shows change in light intensity over time. Data obtained from the temperature and humidity sensor is shown as a separate circular bar (Figure 4). The color of the area graph and the circular bar(s) is changed if the value exceeds a threshold, as shown in figure 4 (right). We also provided haptic feedback on the hands for the same. A video demonstration of the system can be found at https://youtu.be/-UOB9Stgxd8.

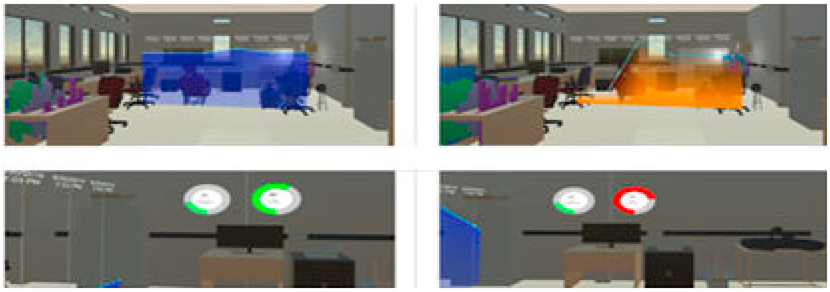

Fig. 4 Visualization of real-time sensor data inside VR Digital Twin

4. User Studies

4.1. Study on 2D Graph Visualization

Aim of the Study: We undertook the following study to investigate how users interpret information from different types of graphs. A similar study was conducted earlier [26], where gaze locations were captured to analyze users' attention to specific parts of the visualization technique. We have developed new techniques for analyzing gaze data based on soft clustering. In particular, we investigated the Expectation-Maximization (EM) algorithm. We have used the XB cluster validation index [10] for validating the optimum number of clusters. We could automatically identify the number and locations of areas of interest in a visual display using these soft clustering techniques. This study will be useful to point the anomalies in the current visualization techniques.

Expectation–Maximization (EM) is an iterative method to find Maximum Likelihood or Maximum a Posteriori (MAP) estimates of parameters in statistical models, where the model depends on unobserved latent variables. The EM iteration alternates between performing an expectation (E) step, which creates a function for the expectation of the log-likelihood evaluated using the current estimate for the parameters. A maximization (M) step computes parameters maximizing the expected log-likelihood found on the *E* step. These parameter estimates are then used to determine the distribution of the latent variables in the next E step.

XB Cluster Validation Index: A cluster validity function proposed by Xie and Beni・ [10] is used to evaluate the fitness of partitions produced by clustering algorithms. It is defined as the compactness measure and separation measure ratio, i.e., lower index value indicates fitter partitions.

Participants: We conducted the user study with 9 participants: six males and three females, everyone between 20 and 35 years.

Materials: We used a Tobii Eye-X tracker for recording eye gaze, a 29-inch display monitor with 1366×768 screen resolution, and a Lenovo Yoga laptop with an i5 processor for conducting the user study. As per the Tobii Eye-X license agreement, we did not store raw eye gaze data; instead, only analyzed data in real-time.

Design: We developed software that consists of four visualization techniques and five sets of questions with multiple choice answers. An eye gaze tracker was placed at the bottom of the screen. Participants were asked to sit at

75 cm away from the screen. They were instructed to answer a set of questions by investigating the graph. Figure 5 shows a sample interface of the system. The four graphs used are bar graph, line graph, radar graph, and area graph. For each graph, the following set of questions were displayed one at a time. The order of presentations of the graphs and questions was randomized to reduce learning and order effects.

Q1: How many sensors have lesser average value than average of all low values?

Q2: Average of which sensor is approximately same as the average of all sensor's average value?

Q3: Sensor having high value greater than 50 and less than 100?

Q4: Two sensor reading showing nearly equal low values with minimum difference?

Q5: What is the approximate average of all High values of sensors?

Procedure: Participants were briefed about the experiment. For each participant, the eye tracker was calibrated using the Tobii calibration routine [27]. After calibration, participants were asked to undertake the study. The X-Y coordinates of the gaze location and response to each question with timestamp were logged in a text file.

Results and Discussion: Our analysis found a significant difference in gaze and response behavior for different graphs while performing similar tasks. We analyzed four dependent variables: the number of correct answers, average time for correct answers, total time taken for all answers, and the optimal number of clusters for the user's gaze fixation. Moreover, we analyzed the user's gaze fixation using the Expectation-Maximization algorithm, which indicates that more fixations mean more eye gaze movement requiring a longer duration to analyze data. We found that Bar graph has the highest number of correct answers with 27 correct answers, and the Radar graph has the lowest with 19 correct answers out of 45 questions, all users cumulatively. Area Graph has the lowest average response time for individual questions (24.6 seconds) and total time for all questions (155.86 seconds). We also noticed that Bar graph's average response time is high, and the number of correct answers for the Area graph is low. This speed-accuracy trade-off may lead us to future research questions. We undertook one-way ANOVA (Analysis of Variance) for all dependent variables and did not find significant differences for any of the dependent variables [p>0.05].

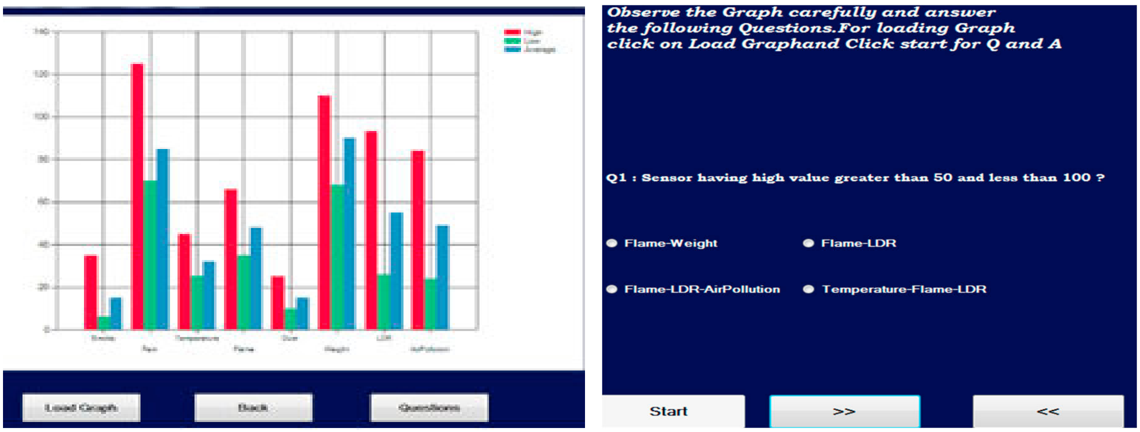

Fig. 5 Graphical and questionnaire interface of the system

Table 1 above shows the average values of all dependent variables for all types of graphs. We analyzed the sequences of eye gaze fixations in all four graphs like Steichen's study [26]. We divided the screen into 9 regions and analyzes first saccade positions and subsequent gaze movements from the initial position. We noted that the user's eye gaze first fixated on the central part and moved to the bottom-center of the graph subsequently for all types of graphs. We also noticed that initial patterns for eye gaze fixations are similar for all graphs. However, subsequent gaze movements are different for each graph. We found after mining those movements that the sequence of bottom-center to middle-center and top-right to middle-center is most frequent among all two-region sequences.

Table I: Values of dependent variables

	Bar	Line	Radar	Area
CA	3	2.22	2.11	2.67
ART (secs)	37.33	30.35	39.45	24.6
TRT (secs)	196.77	166.35	212.83	155.86
ONC	4.55	4.66	3.55	3.55

CA: Number of correct answers
ART: Average Response time for correct answers in seconds
TRT: Total response time for all answers in seconds
ONC: Optimum number of clusters

4.2. Study on 3D Graph Visualization

Aim of the Study: In order to investigate and compare visual variables and charts, we designed and conducted a user study with six types of visualization techniques. Each technique displayed numerical data and nominal data using different combinations of visual variables. In our study, we considered synthetic sensor data and used five different sensors: temperature, humidity, smoke, air, and light. We have three instances of each sensor, and we use the term “node” to refer to all instances of a particular type of sensor. The data type of node was nominal. In total, there are 15 data points and five sensor nodes. We developed and used six types of charts in our study, bar-size/bar chart (BC), bar-orientation (BOR), bar-opacity (BO), shape-size (SS), shape-opacity (SO), and area chart (AC). Nodes were arranged on the x-axis, and instances of each node were arranged in the z-axis for all six charts. The Bar-Size and Area chart are shown in figure 6.

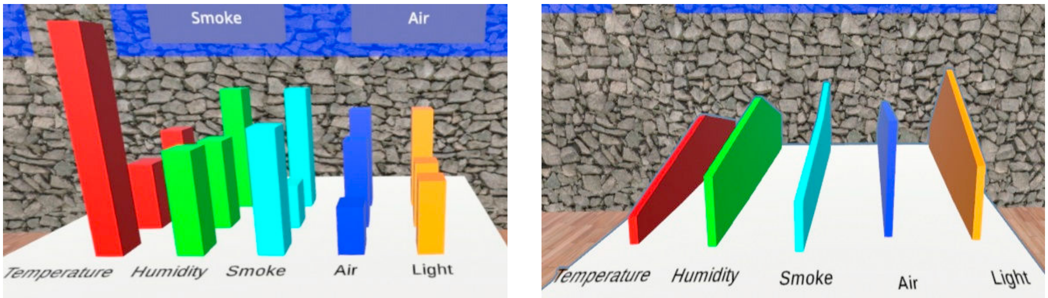

Fig. 6 Bar-Size and Area chart

Analysis Methodology: We next describe algorithms considered for analyzing gaze-based metrics and cognitive load from ocular parameters.

A. **Fixation and saccade rate:** We calculated fixation and saccade rates by detecting fixations and saccades from gaze direction data using the velocity threshold fixation identification method (I-VT) [**33**]. We then calculated fixation and saccade rate as the number of fixations and saccades per second.

B. **Revisit sequences:** A sequence refers to an ordered collection of focused nodes without repetitions. Revisit sequences provide information about how many times a participant scanned through a sequence. This metric allows us to examine graphs that were repeatedly observed. We investigated three types of revisit sequences – sequences of lengths 3, 4, and 5. We also analyzed two parameters of revisit sequences: (i) number of unique sequences and (ii) total revisit sequences.

C. **Low pass filter of pupil (LPF):** We divided the pupil dilation data into sections of 100 samples and subtracted mean from the raw data. We used a Butterworth lowpass filter with a cut-off frequency of 5 Hz [34] and added the magnitude of the filtered data using a running window of size 1-sec with 70% overlap. This algorithm uses a conventional filtering technique in Digital Signal Processing (DSP), which uses time-domain difference equations to filter the signal.

D. **EEG Data:** We used EmotivBCI software to monitor EEG signals and recorded data streams from the EEG headset. The EmotivBCI software automatically calculates power signals for five EEG bands, and we considered alpha, low beta, high beta, and theta bands. We removed outlier from raw EEG data using the inner fence.

Participants: We collected data from 17 participants with an average age of 28 years (male:15 and female: 2) recruited from our university. We took appropriate ethical approval from the university ethics committee for conducting the experiment.

Materials: We used HTC Vive Pro Eye with an inbuilt eye-tracker and refresh rate of 90Hz to collect gaze-based data and pupil diameter (accuracy 0.5 of visual angle). We have also used the Emotiv Insight EEG tracker with five dry electrodes and a sampling rate of 128 Samples per Second (SPS) to collect EEG data. Our computer architecture consists of an Intel Core i5 processor and Nvidia 2070 graphics card.

Design: We designed and set up a VR environment scene using the Unity 3D game engine. The scene consists of a visualization chart and a set of 4 questions. We set questions based on low-level tasks by Amar et al. [35]. A video demonstration of the VR study can be seen at https://youtu.be/y5-Adxk4uVo

Procedure: Participants were briefed about the aim of the study and shown a virtual walkthrough of the environment. We calibrated the hand controller and eye tracker for each participant separately. We proceeded with the trial to select the target, and the proprietary eye-tracking software indicated the calibration to be successful. We instructed participants to use the VR headset for ten minutes to get accustomed to the VR scene. Participants were instructed to move around the scene using a teleport button on the VR hand controller. When participants were comfortable with the scene, we asked them to start the task by wearing both an EEG tracker and HTC Vive Pro Eye. Participants were then requested to observe the visualization chart and answer four questions.

Results and Discussion: We found that both bar-opacity and bar-size charts are similar in terms of correct data interpretation. We then noticed that bar sizes' accuracy per unit time is higher than other charts as shown in figure 7 (left) and requires the least number of revisits. We can infer from these results that a bar-size chart is best in terms of correct data interpretation. We found that color makes it easier to interpret nominal data as compared to shape. The size variable reduces the time required for processing numerical data as compared to the other two variables. The size variable also performs favorably in terms of the count of revisit sequences. We also observed that the addition of the 3rd dimension to the visualization affects the performance of participants. We noticed that the movement of saccades along the z-axis is more than the movement along the y-axis but less than the x-axis as shown in figure 7 (right). Significant differences were noticed among six pairs of charts concerning cognitive load. However, we only found a significant difference between the area chart and bar-size chart in all the three measured bands. We observed that the bar-size chart is incurring less motor action and cognitive load estimated through ocular and EEG parameters [36].

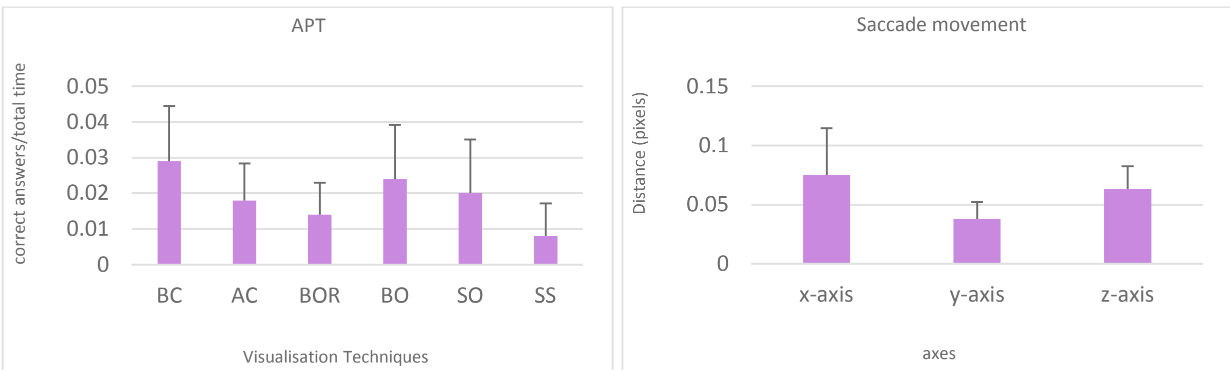

Fig. 7 Results of accuracy per unit time and saccadic movement along three axes

4.3. Study on Effect of Feedback in VR

The previous case study involves optimizing the visual rendering of the 2D sensor dashboard, while the second case study compared visual, haptic, and multimodal feedback in a VR environment. We designed a study inspired by the experiment reported by Fitts [23].

Participants: Twelve participants (nine male and three females; Age range: 23 – 33 years; All right-handed) are recruited for the study. Each prospective participant answered the simulator sickness questionnaire [28]. Even though two participants wanted slightly longer breaks between the study compared to the others, simulator sickness is not a problem in our study. A goniometer is used to verify the degree of hand movement, and all the participants have full range movement.

Materials: We used Unity [29] to design the virtual environment and Oculus Rift [30] system for displaying it. The tracking sensors of Oculus Rift are kept undisturbed throughout the study. We used a desktop with an i7 processor and Nvidia GTX 1080 Ti for this study. Oculus rift right-hand controller is used for performing the task.

Design: We created a virtual environment that resembles the original Fitts' experiment [23]. The environment contains a platform tilted towards the participant. The platform contains two cubes, equidistant from the center. A blue circle has been shown as a representation of the rift controller in the 3D space. We considered three different values for distance between the two cubes (A = 1, 1.5, and 2) and three different values for the width of the cubes (0.05, 0.1, 0.15) on the platform, and hence we have 9 study cases. The index of difficulty (ID) [23] is calculated based on the following equation.

$$ID = log_2\left(\frac{A}{W} + 1\right)$$

The numbers mentioned above have the units same as the default Unity settings. Based on the above choice of distance and widths, we obtained 7 Index of difficulties. Using ID and measured mean movement time for each case, we compute throughput as the ratio of Index of difficulty and mean movement time. The experiment is conducted with four feedback cases.

1. No feedback to the participant.
2. Visual Feedback: The cube turns green as the participant reaches it.
3. Haptic feedback is provided as the participant reaches a cube
    a. Vibrational Haptic feedback is given using the oculus controller and the in-built classes OVRHaptics and OVRHapticsClip (*Haptics*) [31].
4. Both visual and haptic feedback is given once the participant reaches the cube.

Participants were instructed to

1. Bring the controller onto either of the cube on the platform
2. Press "A" button on the controller, drag the controller towards the other cube
3. Release the button.

Movement time in each case is the time between a 'press' and 'release' of the button 'A' on the controller. For a given width of the cube, distance between the cubes, and a feedback case, a participant does the task as mentioned above 25 times. Mean movement time is considered as the average of the movement times over those 25 measurements. If the participant presses or releases the button outside the boundary of the cubes on the platform, it is considered an error and is measured from the nearest edge of the cube.

Procedure: Each participant is instructed to get accustomed to the VR environment, as 8 out of 12 participants experiencing VR for the first time. Then, they answered the simulator sickness questionnaire to ensure that they do not feel uncomfortable during the experiment. The participants are asked to perform the task mentioned above in the VR version of Fitts' experimental setup for around 15 minutes. It is to minimize the learning of the task during the actual trial. Since we considered three widths for the cube, three distances between the cubes, and four feedback cases, we get 36 test cases. These 36 test cases are randomized for each participant. All participants were instructed to do the task "*as quickly and as accurately as possible*." In each trial, mean movement time and errors committed were recorded. Figure 8 shows the VR environment for the visual feedback case. After each participant completes their trial, subjective feedback is collected using NASA TLX for cognitive load and the SUS questionnaire for subjective preference.

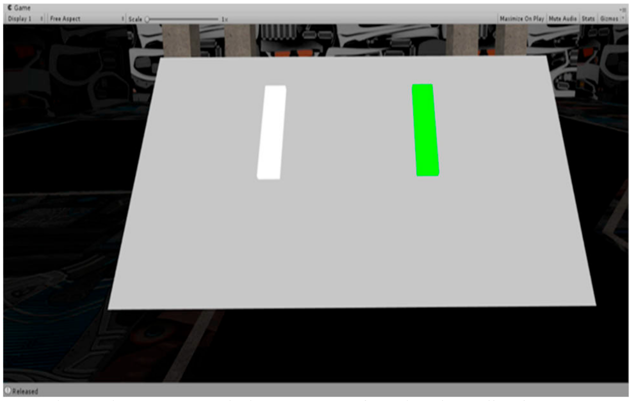

Fig. 8 Fitts' Law Study in VR Setup for Visual Feedback Case

Results and Discussion: Initially, we calculated the average movement time of the hand for each modality. Figure 9 plots the mean movement time with respect to indices of difficulty in each feedback case. In addition to that, the figure also plots the least square fit (LS) line for each feedback case. Except for the visual feedback case, we can observe that the R square values (coefficient of determination) [32] is around 0.9 in all other feedback cases. The lowest movement time was found for Haptic feedback. We undertook one-way ANOVA on movement times but did not find any significant effect. We undertook six pairwise t-tests and found that

- Visual and No-feedback cases needed significantly higher ($p<0.05$) movement times than haptic and multimodal feedback cases.
- Haptic feedback needed significantly lower time than multimodal feedback case.
- There was no significant difference between visual and no-feedback cases.

We also undertook one-way ANOVA on TLX scores but did not find any significant effect. For pairwise t-tests we found that

- In Visual and Multimodal cases, participants have experienced significantly lower ($p<0.05$) cognitive load than no feedback case.
- Participants experienced significantly lower cognitive load in multimodal feedback case than in visual and haptic feedback cases.
- The experienced cognitive load in haptic feedback case is not significantly different from no-feedback and visual feedback cases.

An one way ANOVA for SUS scores found significant difference among different feedback cases $F(3,44) = 5.4$, $p<0.05$, $\eta2 = 0.27$. Six pairwise t-tests found that

- Subjective preference to Visual and Multimodal feedback cases is significantly higher ($p<0.05$) than to a No Feedback case.
- Preference towards multimodal feedback is significantly higher than to haptic feedback.
- Preference towards a multimodal feedback than to a visual feedback is not significantly different.
- Preference towards no feedback and visual feedback is not significantly different from a haptic feedback case.

The grey shaded regions in Table II signify the cases with the statistically significant improvement compared to the baseline no-feedback case. The results infer that quantitatively haptic and multimodal have higher throughput, and users prefer qualitatively multimodal and visual feedback.

Table II: Quantitative and Qualitative Results of VR Fitts' Study

Feedback Type	Mean Movement Time (ms)	Mean Throughput (bits/sec)	Mean Error	Mean SUS	Mean TLX
No Feedback	665.01 (94.52)	6.107 (0.48)	1.07 (0.28)	58.13 (12.9)	49.41 (18.1)
Visual	670.39 (96.74)	6.05 (0.53)	1.09 (0.28)	75.42 (14.7)	36.94 (18.1)
Haptic	613.23 (86.67)	6.64 (0.44)	1.06 (0.29)	65.41 (14.6)	43.26 (16.2)
Multimodal (Visual and Haptic)	641.65 (87.02)	6.33 (0.52)	1.06 (0.28)	78.33 (13)	30.11 (16.6)

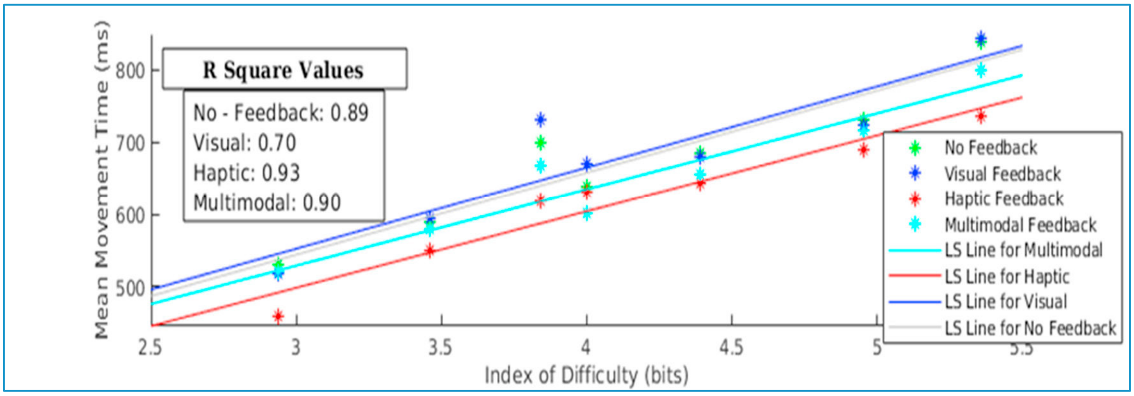

Fig. 9 Mean Movement Time Vs Index of Difficulty for various feedback cases augmented with a least-squares line

5. Conclusions and Future work

This paper presents the development of a smart sensor dashboard having both 2D and 3D visualization modules. It describes different modules of the sensor dashboard and presents two user studies on analyzing existing visualization techniques in 2D and 3D. We also studied various feedback cases in the case of the 3D virtual sensor dashboard. From the gaze fixation analysis for existing visualization techniques in 2D, we observed that initial patterns for eye gaze fixations are similar for all graphs. However, subsequent gaze movements are different for each graph. We found after mining those movements that the sequence of bottom-center to middle-center and top-right to middle-center is most frequent among all two-region sequences. In a 3D visualization study, we found that a bar chart with different size columns for data points values were found to generate the most accurate response and least cognitive load among users.

In the VR sensor dashboard study, we studied the interaction paradigm across four feedback cases. We observed that the users perceived multimodal visual and haptic feedback better on qualitative and quantitative analysis. We take these results forward for interaction design in the case of 3D visualization. We shall study and compare the results and efficacy of the 3D visualization experiment against the results we obtained for the 2D visualization scenario. Since the walk-through of a virtual room with live sensor nodes is already designed, we shall conduct experiments to evaluate the efficacy of these dynamic sensor dashboards against static screen dashboards. The application we envisage as a result of our future work at this moment is a virtual smart factory application using which a person can inspect and interact with every entity of the smart virtual factory to retrieve information and to discharge commands.

References

[1] Vrba, P., Kadera, P., Jirkovský, V., Obitko, M., & Mařík, V. (2011, August). New trends of visualization in smart production control systems. In International Conference on Industrial Applications of Holonic and Multi-Agent Systems (pp. 72-83). Springer, Berlin, Heidelberg.
[2] Sarkar, B., Chakrabarti, A., & Ananthasuresh, G. K. (2015). Synthesis of conceptual designs for sensors using SAPPhIRE-lite. In DS 80-5 Proceedings of the 20th International Conference on Engineering Design (ICED 15) Vol 5: Design Methods and Tools-Part 1, Milan, Italy, 27-30.07. 15 (pp. 115-124).
[3] Sackett, P. J., Al-Gaylani, M. F., Tiwari, A., & Williams, D. (2006). A review of data visualization: opportunities in manufacturing sequence management. International Journal of Computer Integrated Manufacturing, 19(7), 689-704.
[4] Jolliffe, I. (2011). Principal component analysis (pp. 1094-1096). Springer Berlin Heidelberg.
[5] Torgerson, W. S. (1952). Multidimensional scaling: I. Theory and method. Psychometrika, 17(4), 401-419.
[6] Inselberg, A., & Dimsdale, B. (1990, October). Parallel coordinates: a tool for visualizing multi-dimensional geometry. In Proceedings of the 1st conference on Visualization'90 (pp. 361-378). IEEE Computer Society Press.
[7] Chernoff, H. (1973). The use of faces to represent points in k-dimensional space graphically. Journal of the American Statistical Association, 68(342), 361-368.
[8] Ellis, G., & Dix, A. (2007). A taxonomy of clutter reduction for information visualisation. IEEE transactions on visualization and computer graphics, 13(6), 1216-1223.
[9] Hoffman, P. E., & Grinstein, G. G. (2002). A survey of visualizations for high-dimensional data mining. Information visualization in data mining and knowledge discovery, 104, 4.
[10] Bertini, E., Tatu, A., & Keim, D. (2011). Quality metrics in high-dimensional data visualization: An overview and systematization. IEEE Transactions on Visualization and Computer Graphics, 17(12), 2203-2212.
[11] Fuchs, R., & Hauser, H. (2009, September). Visualization of multi□variate scientific data. In Computer Graphics Forum (Vol. 28, No. 6, pp. 1670-1690). Oxford, UK: Blackwell Publishing Ltd.
[12] Kehrer, J., & Hauser, H. (2012). Visualization and visual analysis of multifaceted scientific data: A survey. IEEE transactions on visualization and computer graphics, 19(3), 495-513.
[13] Chan, W. W. Y. (2006). A survey on multivariate data visualization. Department of Computer Science and Engineering. Hong Kong University of Science and Technology, 8(6), 1-29.
[14] Munzner, T. (2015). Visualization Analysis and Design. CRC Press. ISBN: 9781498759717.
[15] Blumenschein, M., Behrisch, M., Schmid, S., Butscher, S., Wahl, D. R., Villinger, K., ... & Keim, D. A. (2018). SMARTexplore: Simplifying High-Dimensional Data Analysis through a Table-Based Visual Analytics Approach. In IEEE Conference on Visual Analytics Science and Technology (VAST) 2018.
[16] Bolt, R. A. (1980). "Put-that-there": Voice and gesture at the graphics interface (Vol. 14, No. 3, pp. 262-270). ACM.
[17] Cohen, P. R., Johnston, M., McGee, D., Oviatt, S. L., Pittman, J., Smith, I. A., ... & Clow, J. (1997, November). QuickSet: Multimodal Interaction for Distributed Applications. In ACM Multimedia (Vol. 97, pp. 31-40).
[18] Koons, D. B., Sparrell, C. J., & Thorisson, K. R. (1993). Integrating simultaneous input from speech, gaze, and hand gestures. MIT Press: Menlo Park, CA, 257-276.
[19] Neal, J. G., Thielman, C. Y., Dobes, Z., Haller, S. M., Glanowski, S., & Shapiro, S. C. (1989). CUBRICON: a multimodal user interface. In GIS/LIS'89.
[20] Erler, P. (2017). Haptic Feedback in Room-Scale VR (Institute of Computer Graphics and Algorithms, Vienna University of Technology). Available: https://www.cg.tuwien.ac.at/research/publications/2017/ERLER-2017-HVR/ . Accessed on 01-Aug-2019
[21] Biswas, P., Roy, S., Prabhakar, G., Rajesh, J., Arjun, S., Arora, M., ... & Chakrabarti, A. (2017, July). Interactive sensor visualization for smart manufacturing system. In Proceedings of the 31st British Computer Society Human Computer Interaction Conference (p. 99). BCS Learning & Development Ltd..
[22] Arjun, S. (2018, July). Personalizing data visualization and interaction. In Adjunct Publication of the 26th Conference on User Modeling, Adaptation and Personalization (pp. 199-202). ACM.
[23] Fitts, P. M. (1954). The information capacity of the human motor system in controlling the amplitude of movement. Journal of experimental psychology, 47(6), 381.
[24] Espressif Systems (2019). ESP-WROOM-02 Overview. Available: https://www.espressif.com/en/products/hardware/esp-wroom-02/overview. Accessed on 20-Aug-2019
[25] BitSplash Interactive.(2019). Graph and Chart. Available: https://assetstore.unity.com/packages/tools/gui/graph-and-chart-78488. Accessed on 20-Aug-2019
[26] Steichen, B., Wu, M. M., Toker, D., Conati, C., & Carenini, G. (2014, July). Te, Te, Hi, Hi: Eye gaze sequence analysis for informing user-adaptive information visualizations. In International Conference on User Modeling, Adaptation, and Personalization (pp. 183-194). Springer, Cham.
[27] Tobii Calibration routine: http://developer.tobiipro.com/commonconcepts/calibration.html
[28] Kennedy, R. S., Lane, N. E., Berbaum, K. S., & Lilienthal, M. G. (1993). Simulator sickness questionnaire: An enhanced method for quantifying simulator sickness. The international journal of aviation psychology, 3(3), 203-220.
[29] Unity(2019). Unity Available: https://unity.com/. Accessed on 10-April-2019
[30] Oculus Rift: VR Headset for VR Ready PCs.(2019).Oculus. Available: https://www.oculus.com/rift/. Accessed on 10-April-2019
[31] Haptics.(2019).Available: https://developer.oculus.com/documentation/unity/latest/concepts/unity-haptics/. Accessed on 10-April-2019
[32] Hughes, A., & Grawoig, D. (1971). Statistics; a foundation for analysis (No. 311.2 H83).
[33] Salvucci, D. D., & Goldberg, J. H. (2000, November). Identifying fixations and saccades in eye-tracking protocols. In Proceedings of the 2000 symposium on Eye tracking research & applications (pp. 71-78).

[34] Onorati, F., Barbieri, R., Mauri, M., Russo, V., & Mainardi, L. (2013, July). Reconstruction and analysis of the pupil dilation signal: Application to a psychophysiological affective protocol. In 2013 35th Annual International Conference of the IEEE Engineering in Medicine and Biology Society (EMBC) (pp. 5-8). IEEE.
[35] Amar, R., Eagan, J., Stasko, J.: Low-Level Components of Analytic Activity in Information Visualization. In: Proc. of 2005 Symp. on Information Visualization, pp. 15–21 (2005)
[36] Arjun S, Rajshekar GS, Mukhopadhyay A, Vinod S and Biswas P, Evaluating Visual Variables in a Virtual Reality Environment, British HCI 2021